



Recovery from Acute SARS-CoV-2 Infection and Development of Anamnestic Immune Responses in T Cell-Depleted Rhesus Macaques

 Kim J. Hasenkrug,^a Friederike Feldmann,^b Lara Myers,^a Mario L. Santiago,^c Kejun Guo,^c Bradley S. Barrett,^c Kaylee L. Mickens,^c Aaron Carmody,^d  Atsushi Okumura,^e Deepashri Rao,^a Madison M. Collins,^a Ronald J. Messer,^a Jamie Lovaglio,^b Carl Shaia,^b Rebecca Rosenke,^b Neeltje van Doremalen,^e Chad Clancy,^b Greg Saturday,^b Patrick Hanley,^b Brian J. Smith,^b Kimberly Meade-White,^e W. Lesley Shupert,^e David W. Hawman,^e  Heinz Feldmann^e

^aLaboratory of Persistent Viral Diseases, Rocky Mountain Laboratories, National Institute of Allergy and Infectious Diseases, National Institutes of Health, Hamilton, Montana, USA

^bRocky Mountain Veterinary Branch, Rocky Mountain Laboratories, National Institute of Allergy and Infectious Diseases, National Institutes of Health, Hamilton, Montana, USA

^cDepartments of Medicine, Immunology and Microbiology, University of Colorado School of Medicine, Aurora, Colorado, USA

^dResearch Technologies Branch, Rocky Mountain Laboratories, National Institute of Allergy and Infectious Diseases, National Institutes of Health, Hamilton, Montana, USA

^eLaboratory of Virology, Rocky Mountain Laboratories, National Institute of Allergy and Infectious Diseases, National Institutes of Health, Hamilton, Montana, USA

ABSTRACT Severe coronavirus disease 2019 (COVID-19) has been associated with T cell lymphopenia, but no causal effect of T cell deficiency on disease severity has been established. To investigate the specific role of T cells in recovery from severe acute respiratory syndrome coronavirus 2 (SARS-CoV-2) infections, we studied rhesus macaques that were depleted of either CD4⁺, CD8⁺, or both T cell subsets prior to infection. Peak virus loads were similar in all groups, but the resolution of virus in the T cell-depleted animals was slightly delayed compared to that in controls. The T cell-depleted groups developed virus-neutralizing antibody responses and class switched to IgG. When reinfected 6 weeks later, the T cell-depleted animals showed anamnestic immune responses characterized by rapid induction of high-titer virus-neutralizing antibodies, faster control of virus loads, and reduced clinical signs. These results indicate that while T cells play a role in the recovery of rhesus macaques from acute SARS-CoV-2 infections, their depletion does not induce severe disease, and T cells do not account for the natural resistance of rhesus macaques to severe COVID-19. Neither primed CD4⁺ nor CD8⁺ T cells appeared critical for immunoglobulin class switching, the development of immunological memory, or protection from a second infection.

IMPORTANCE Patients with severe COVID-19 often have decreased numbers of T cells, a cell type important in fighting most viral infections. However, it is not known whether the loss of T cells contributes to severe COVID-19 or is a consequence of it. We studied rhesus macaques, which develop only mild COVID-19, similar to most humans. Experimental depletion of T cells slightly prolonged their clearance of virus, but there was no increase in disease severity. Furthermore, they were able to develop protection from a second infection and produced antibodies capable of neutralizing the virus. They also developed immunological memory, which allows a much stronger and more rapid response upon a second infection. These results suggest that T cells are not critical for recovery from acute SARS-CoV-2 infections in this model and point toward B cell responses and antibodies as the essential mediators of protection from re-exposure.

KEYWORDS SARS-CoV-2, T cells, macaque, neutralizing antibodies

Citation Hasenkrug KJ, Feldmann F, Myers L, Santiago ML, Guo K, Barrett BS, Mickens KL, Carmody A, Okumura A, Rao D, Collins MM, Messer RJ, Lovaglio J, Shaia C, Rosenke R, van Doremalen N, Clancy C, Saturday G, Hanley P, Smith BJ, Meade-White K, Shupert WL, Hawman DW, Feldmann H. 2021. Recovery from acute SARS-CoV-2 infection and development of anamnestic immune responses in T cell-depleted rhesus macaques. *mBio* 12:e01503-21. <https://doi.org/10.1128/mBio.01503-21>.

Editor Maria Gloria Dominguez Bello, Rutgers, The State University of New Jersey

This is a work of the U.S. Government and is not subject to copyright protection in the United States. Foreign copyrights may apply.

Address correspondence to Kim J. Hasenkrug, khasenkrug@nih.gov.

This article is a direct contribution from Kim J. Hasenkrug, a Fellow of the American Academy of Microbiology, who arranged for and secured reviews by Dennis Burton, The Scripps Research Institute, and David O'Connor, University of Wisconsin-Madison.

Received 25 May 2021

Accepted 21 June 2021

Published 27 July 2021

Several lines of evidence suggest that T cells play important roles in coronavirus disease 2019 (COVID-19). For example, it has been shown that COVID-19 patients develop both CD4⁺ and CD8⁺ T cells responsive to severe acute respiratory coronavirus 2 (SARS-CoV-2) antigens (1–4), and some T cell phenotypes, such as exhaustion and dysregulation, have been associated with more severe disease (5–9). Also, severe COVID-19 has been associated with lymphopenia (10–12) including loss of both CD4⁺ and CD8⁺ T cells. However, it is not known whether lymphopenia contributes to severe COVID-19 or is a consequence of the disease. Thus, definitive proof of the importance of T cells in recovery from infection and the development of anamnestic (memory) responses remains an open question. As an experimental approach to answer this question, we studied adult rhesus macaques that had been depleted of either CD4⁺, CD8⁺, or both T cell subsets prior to infection with SARS-CoV-2 (Fig. 1a). Similar to most adult humans, rhesus macaques become only mildly or moderately ill following infection with SARS-CoV-2, and they do not normally develop acute respiratory distress syndrome (13, 14). Understanding the immunological mechanisms that participate in the resistance of these animals to severe disease is of great interest because it could lead to the rational design of improved vaccines, prophylactics, and therapeutics. In this study, we focused on the role of T cells in the resolution of acute SARS-CoV-2 infection and in the development of immunological memory which provides better protection upon reinfection. It has been shown that rhesus macaques are protected from reinfection (15, 16), but the role of T cells and particularly CD4⁺ T cells in that protection is not yet fully understood (17).

RESULTS

All macaques were inoculated on day 0 with the Washington isolate of SARS-CoV-2 as previously described (13) and then rested for 6 weeks. The animals were then challenged a second time as previously described. Two separate experiments were carried out, each with three animals per group for a total of six macaques per group. All results from individual animals are labeled with the same symbol in the figures: black symbols represent animals in the first experiment and orange symbols represent those in the second. Findings from the reinfection are highlighted in yellow in the figures.

Lymphocyte responses in normal control animals. Most of the nondepleted control animals showed a rapid but transient lymphopenia with loss of CD4⁺ T helper cells, CD8⁺ T cells and B cells from the blood, possibly due to homing to lymphoid tissues. CD4⁺ T numbers rebounded to approximately equivalent or higher levels by 7 days postinfection (dpi) (Fig. 1b) and CD8⁺ T cell counts were significantly higher at 7 dpi than at day 0 (Fig. 1c), which suggested that cells became mobilized from tissues and entered the bloodstream or that there was a proliferative response to infection. In support of a proliferative response at 7 dpi, circulating CD8⁺ T cells showed a significant increase in cell surface expression of Ki-67, which marks recently proliferated cells (Fig. S1a). Similar responses were observed following reinfection (yellow shading). B cell numbers in the blood also decreased rapidly after infection and then rebounded over the next several weeks (Fig. 1d).

Lymphocyte responses in CD4-depleted animals. At day 0, the CD4⁺ T cell depletion in the blood was greater than 90% in all but one animal (animal CD4-5 was 78% depleted) (Fig. 1e). No significant increases in CD4⁺ T cell numbers were observed in the six subsequent weeks, suggesting that little or no immunological priming occurred. Most animals showed slight increases in CD4⁺ T cell counts following reinfection, but it is not known if this was a response to infection or simply reconstitution following depletion (Fig. 1e, yellow shading). The CD8⁺ T cell responses to both infections were quite similar to those of the controls (Fig. 1f), but there was no B cell response apparent in the blood except for a minimal response by animal CD4-5 following reinfection (Fig. 1g). The reduction of B cell numbers in the CD4-depleted groups compared to the controls over time was statistically significant ($P=0.0118$). Thus, depletion of CD4⁺ T cells produced only a minimal impact on CD8⁺ T cell responses but had a significant negative impact on B cell responses.

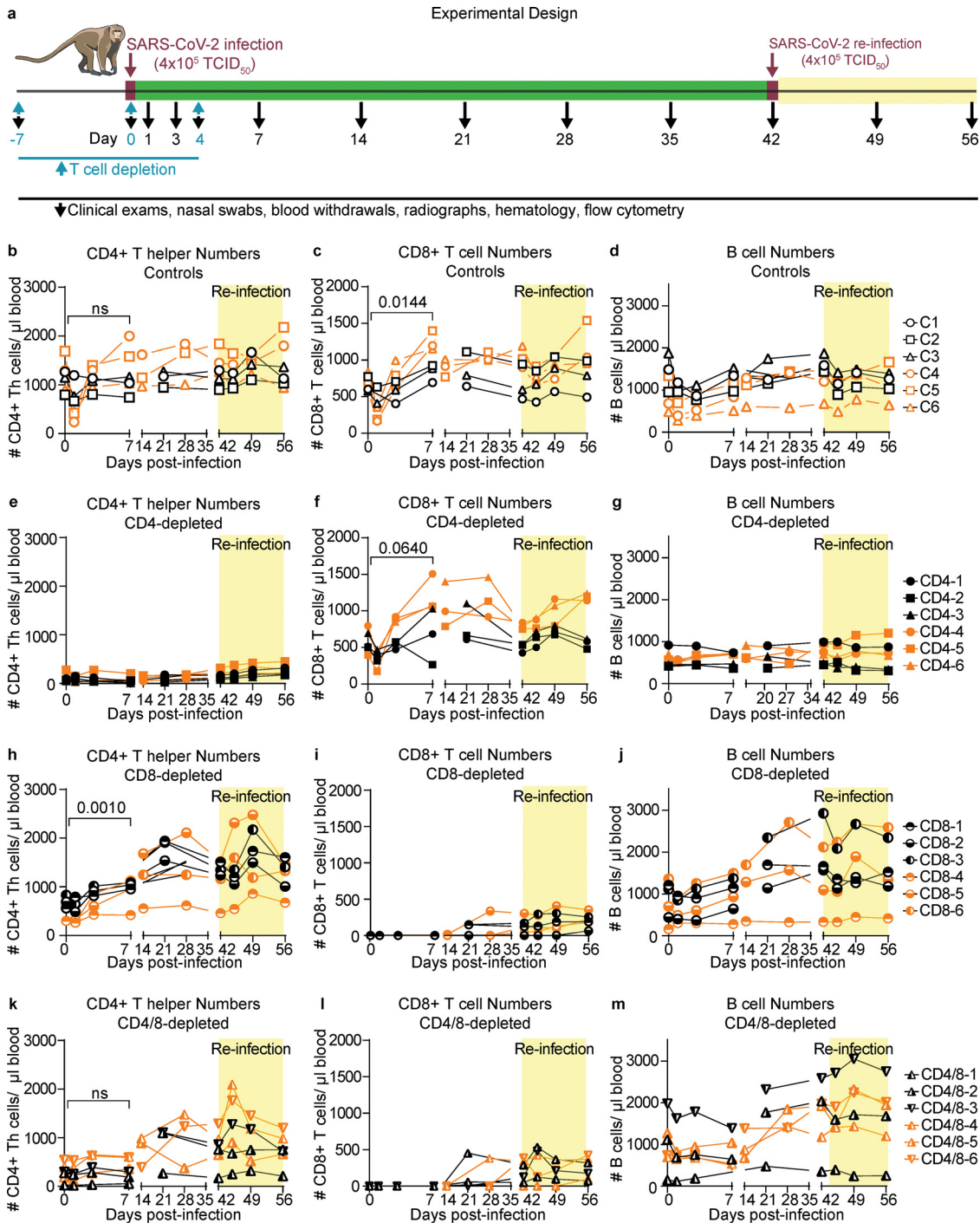


FIG 1 Experimental design and T cell depletions. (a) T cell subset-depleting antibodies were administered on days -7 , 0 , and $+4$, as indicated by blue arrows. Infections were done on days 0 and 42 , as indicated by red arrows. Blood withdrawals were performed on the days indicated by the black arrows, and flow cytometry was used to determine the lymphocyte subset numbers over time. The flow cytometry gating strategies are shown in Fig. S1b. Each symbol represents a single animal throughout. All CD4-depleted animals except CD4-5 were still more than 90% depleted of CD4⁺ T cells at 7 dpi. CD4-5 was 78% depleted. CD4⁺ Th numbers excluded FoxP3⁺ cells. At 7 days after reinfection (49 dpi), the animals averaged 81% depletion. All CD8-depleted animals were >99% depleted at 7 dpi and remained 78% depleted at 49 dpi. The differences between subset numbers at 0 dpi and 7 dpi were calculated by a two-way paired *t* test. ns, not significant. *P* values are shown. Numbers of B cells (d, g, j, and m) were determined by flow cytometry using CD45 and CD20 as markers. The numbers of B cells in the CD4-depleted group were significantly lower over time than those in the controls, as determined by mixed-effects analysis (*P* = 0.0118).

Lymphocyte responses in CD8-depleted animals. The expansion of CD4⁺ T helper cells in the blood following infection in the CD8-depleted animals was similar to that in the controls, although one animal (CD8-4) failed to respond (Fig. 1h). The CD4⁺ T responses to the second infection in a few animals appeared slightly stronger than those in the controls, possibly a compensatory response to the lack of CD8⁺ T cells (Fig. 1h). The CD8⁺ T cell depletions were >99% effective in all animals, and there was no detectable CD8⁺ T cell expansion in the blood for the first 2 weeks after infection, suggesting that minimal or no immunological priming had occurred (Fig. 1i). There was a slight rebound of CD8⁺ T cells in most animals by the day of reinfection but little expansion in the following 2 weeks. Thus, there was no indication of a significant CD8⁺ T cell response to either the first or second infection in the CD8-depleted animals. All but one animal (CD8-4) had B cell expansions as good as or better than those of the controls (Fig. 1j). The one nonresponding animal started the experiment with the lowest CD4⁺ T cell count (Fig. 1h), consistent with the finding that CD4⁺ T cells were important for B cell expansion.

Lymphocyte responses in CD4/CD8-depleted animals. The simultaneous depletions of both CD4⁺ and CD8⁺ T cells were less effective for CD4⁺ T cells than the single-subset depletions and ranged between 56% and 98% at the time of infection (Fig. 1k). The most strongly depleted animal (CD4/8-1) displayed little CD4⁺ T cell responsiveness to either the first or second infection. The other five animals showed delayed CD4⁺ T cell responses compared to controls, but then increased numbers appeared in the 2 to 4 weeks following infection. Four of the animals showed rapid CD4⁺ T cell expansion following reinfection, indicating that the cells had been primed (Fig. 1k). The CD8 depletions were more than 99% effective at 7 dpi (Fig. 1l), and both the CD8⁺ T cell responses and B cell responses (Fig. 1m) were very similar to those in the CD8-depleted group. The one animal that failed to make a B cell response was once again the one with the lowest CD4⁺ T cell numbers (CD4/8-1).

Virus loads. As previously described for SARS-CoV-2-infected macaques (13), all animals had high loads of viral RNA (viral genomes) in nasal swabs, indicative of upper respiratory tract infection. The titers of individual animals in each group are shown in Fig. 2a to d. The RNA loads during the first 2 weeks of infection were not significantly different between groups, but all control animals cleared infections by 14 days, while the T cell-depleted groups did not totally clear until day 21 or later. The dually depleted animals cleared total viral RNA significantly more slowly than the control animals ($P=0.0362$) (Fig. 2d). In all T cell-depleted groups, the second infection was handled better than the first, as evidenced by lower viral RNA loads and quicker resolution (Fig. 2a to d, yellow shading). To minimize detection of residual inoculum, nasal swabs were also tested for viral E gene subgenomic mRNA (sgRNA) indicative of replicating virus (15). The mean loads of sgRNA (Fig. 2a to d, in blue) were lower than the mean loads of total viral RNA but followed similar curves (Fig. 2e to h). Again, all control animals had undetectable sgRNA at 7 dpi, while all T cell-depleted groups still had positive animals. This delay in virus clearance indicated the involvement of CD4⁺ and CD8⁺ T cells in the rapid resolution of acute infection. However, T cells were not essential for eventual clearance. Viral replication in the lower respiratory tract was assayed by testing for sgRNA in bronchoalveolar lavage (BAL) fluid at 1 dpi and at 1 day after reinfection (dpri; 1 dpri=43 dpi). At 1 dpi, all but one control animal had high viral sgRNA loads, with no significant differences between groups (Fig. 2i to l). Upon reinfection, the lungs showed significantly reduced viral sgRNA at 1 dpri compared to 1 dpi, but most animals in all groups had detectable sgRNA in BAL fluid following reinfection. No significant differences between groups were observed at either time point. One or two animals in each group had detectable viral RNA in rectal swabs, but no animals had detectable viral RNA in the blood, consistent with previous reports (13) (data not shown). The improved control of virus in the upper and lower respiratory tracts upon reinfection indicated the presence of anamnestic immune responses, and the similarity of all groups in controlling the second infection indicated that such responses were not dependent on an intact T cell repertoire. We next analyzed clinical signs to

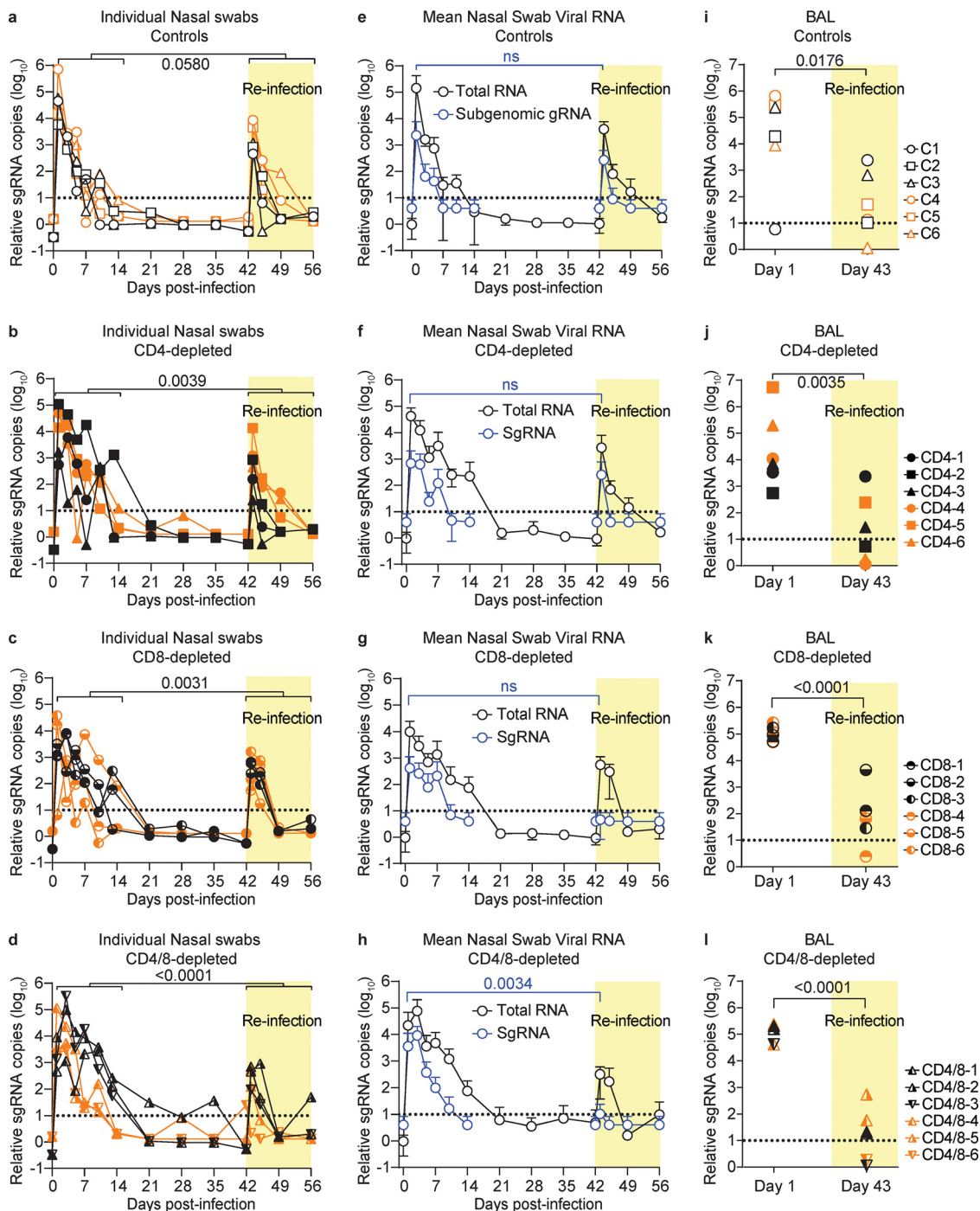


FIG 2 Virus detection from nasal swabs and Broncho-alveolar lavages. (a to d) Each symbol represents the value of viral RNA copies from an individual animal at each time point. The brackets delineate comparisons of cumulative values from the first 2 weeks after infection with those from the 2 weeks after reinfection, and numbers *P* values from two-way paired *t* tests showing significantly reduced virus levels following the second infection (b to d) except in the control group (a), for which the difference was marginally nonsignificant. The cumulative RNA titers from the CD4- and CD8-depleted groups for the first 2 weeks after initial infection were not significantly different from those from the controls, but the CD4/CD8-depleted group had significantly higher titers (*P*=0.0362 by one-way analysis of variance (ANOVA) with a Dunnett's posttest). (e to h) Mean values comparing the total viral RNA data from panels a to d (black lines) with sgRNA results (blue lines). (i to l) Bronchoalveolar lavage fluids were taken at 1 day after infection and reinfection. sgRNA was measured from each animal and showed significantly reduced virus replication upon second infection (*P* values from paired *t* tests are shown).

determine if the reduced viral loads following reinfection were associated with reduced disease.

Clinical signs. On exam days, each animal was scored in a blinded manner for clinical signs and pulmonary radiographs were performed. The most common clinical signs were reduced appetite, slightly irregular abdominal breathing, ruffled fur, and pale appearance (Table S1). The cumulative clinical scores for each animal during the first 2 weeks of infection and reinfection are shown in Fig. 3a to d. All animals developed mild and transient clinical signs during acute infection, and there were no significant differences between the groups. Of note, it cannot be excluded that some of the clinical signs were in response to the procedures performed on the animals, which included anesthesia, blood withdrawals, intratracheal virus inoculation, and bronchoalveolar lavage. However, upon reinfection, the animals underwent the same procedures, and the mean clinical scores in all groups were significantly reduced compared to those in primary infection (Fig. 3a to d, yellow shading). Pulmonary radiographs showed that all animals developed minor lesions in at least one lobe of the lungs during the first infection (Fig. 3e to h), and the scores were significantly lower after reinfection except in the CD8-depleted group. There were no statistically significant differences in the radiological findings between the control animals and the depleted animals at any time points. We thought it worth noting that all of the control animals and four of six CD4-depleted animals developed a rapid but transient blood neutrophilia following the first but not the second infection (Fig. 3i). Neutrophilia may result from the stress of handling the animals, but no significant neutrophilia was observed following the first infection in either the CD8-depleted or dually depleted animals (Fig. 3k and l). These findings suggested that neutrophilia was CD8⁺ T cell dependent. As a whole, these results indicated that neither CD4⁺ nor CD8⁺ T cells appeared critical for either recovery from the first infection or improved control of the second infection. Furthermore, there was no evidence that T cell-mediated immunopathology was involved in the disease. The decreased clinical signs following the second infection indicated the induction of an anamnestic immune response that appeared to be largely independent of T cells. Thus, it was of interest to next investigate the antibody responses.

Antibody responses. (i) Controls. The development of SARS-CoV-2 receptor binding domain (RBD)-binding antibodies was analyzed in a kinetic manner. The first antibody subtype that develops in response to infections is IgM, and all control animals produced RBD-specific IgM responses peaking at 14 dpi (Fig. 4a). During the antibody maturation process, class switch recombination leads to the development of IgG isotype antibodies in a process that is usually dependent on CD4⁺ T cells. As expected, IgG responses also developed, lagging behind the IgM responses by 1 to 2 weeks and peaking in most animals at 4 weeks postinfection (Fig. 4b). Of note, the IgG titers had waned slightly by 6 weeks postinfection. Upon reinfection, IgG titers rose quickly and dramatically, with a mean 37-fold increase in titer within 1 week (Fig. 4b). All control animals also developed virus-neutralizing antibody (nAb) responses with kinetics similar to those of the RBD-specific IgG responses (Fig. 1c). These results demonstrated a strong anamnestic antibody response.

(ii) CD4-depleted animals. Half of the CD4-depleted animals showed delayed or flat IgM responses (Fig. 4d), and two of them also showed flat IgG responses until reinfection (Fig. 4e). More surprising was that the other four animals developed class-switched IgG responses and all of them developed both virus-neutralizing responses (Fig. 4f) and strong anamnestic responses upon reinfection (Fig. 4e). One of the animals in the CD4-depleted group (CD4-2) started the experiment with IgM cross-reactive with RBD (Fig. 4d), as did one of the CD8-depleted animals (CD8-3). This may have been due to a previous exposure to a different coronavirus. Overall, CD4 depletion delayed and/or dampened IgM and IgG responses in some animals, but all animals developed strong anamnestic IgG responses upon reinfection.

(iii) CD8- and CD4/CD8-depleted animals. The IgM, IgG, and nAb responses of both the CD8-depleted (Fig. 4g to i) and CD4/CD8-depleted (Fig. 4j to l) animals can be

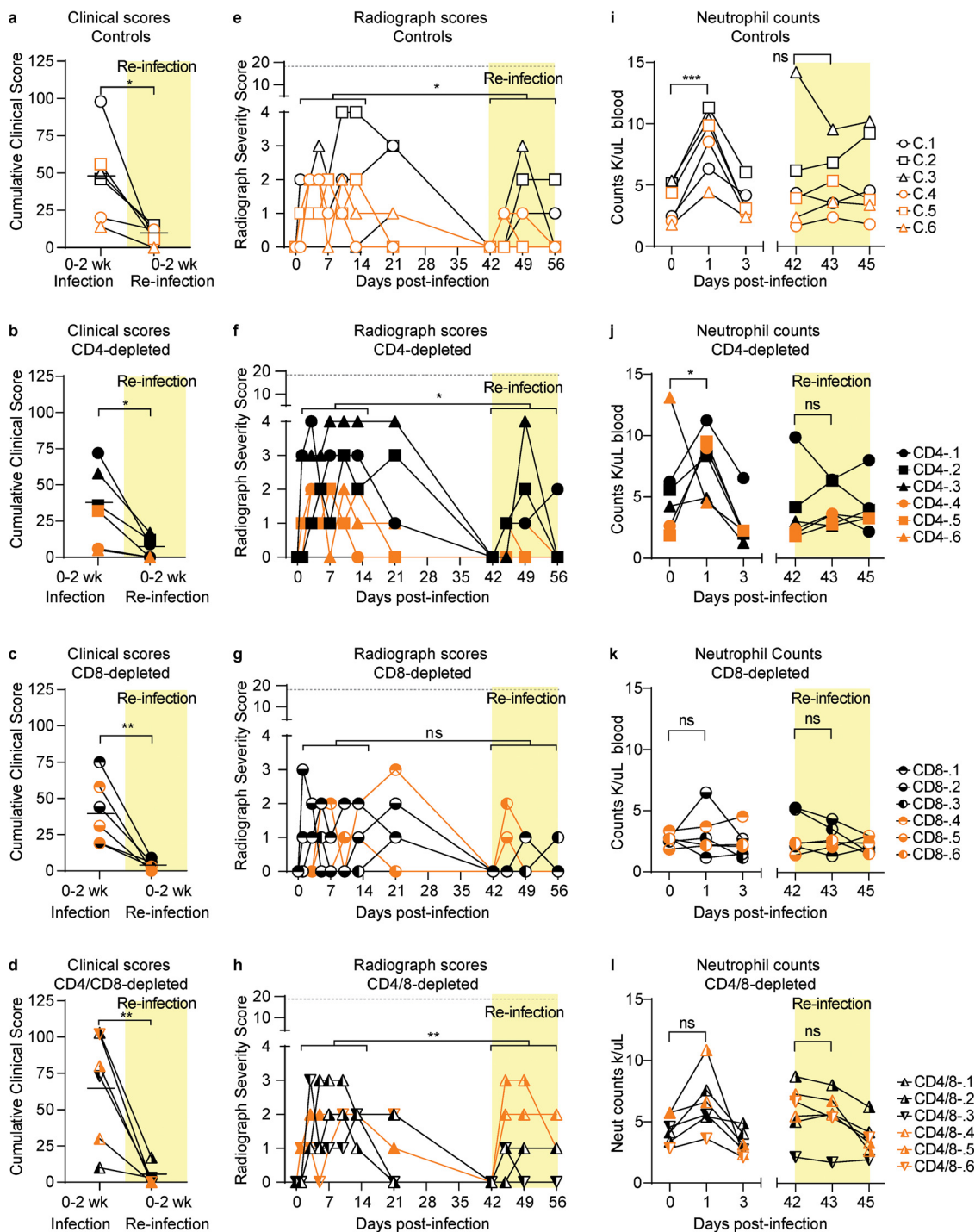


FIG 3 Clinical and radiograph scores and neutrophil counts. (a to d) Clinical signs were scored in a blind manner using a clinical score sheet. Cumulative scores for the 2 weeks following the first infection were compared with the 2 weeks following reinfection (yellow shading) using a two-way paired Student's *t* test. The dashed lines indicate means. (e to h) Radiographs were scored in a blind manner for the presence of pulmonary infiltrates by two board-certified clinical veterinarians. Cumulative scores were analyzed as for panels a to d. The dotted line indicates the maximum score if all lobes were severely affected. (i to l) Neutrophil counts for each animal were taken on blood withdrawal days, and significant differences were noted only between days 0 and 3, as shown. ns, not significant; *, *P* < 0.05; **, *P* < 0.01; ***, *P* < 0.001.

summarized as being very similar to each other and to those of the controls. No significant effect of CD8 depletions on antibody responses was observed.

In summary, there was no major impact of T cell depletions on the antibody responses even though there was no detectable B cell response in the blood of the

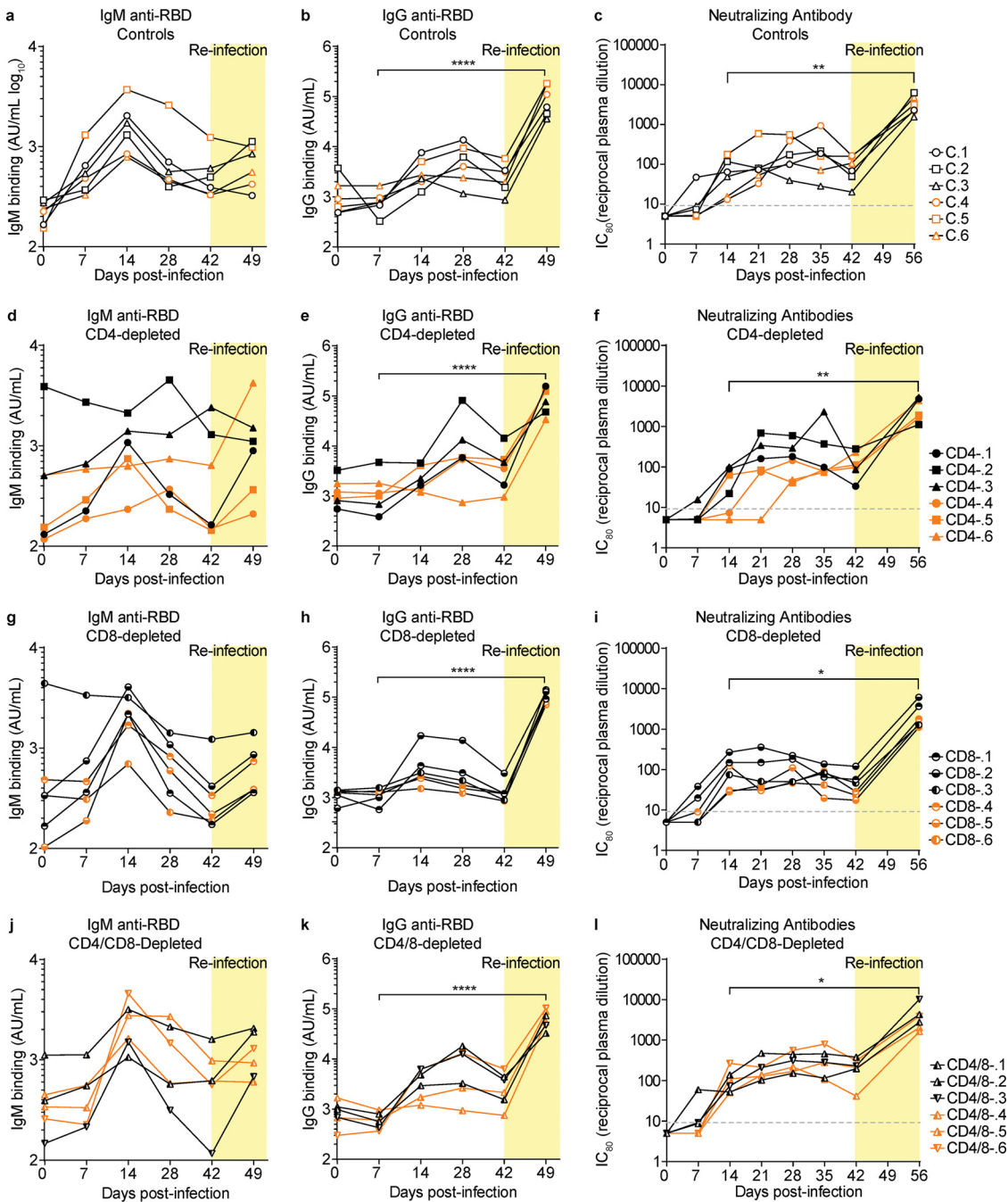


FIG 4 Antibody responses. SARS-CoV-2 spike receptor binding domain-specific IgM (a, d, g, and j) and IgG responses (b, e, h, and k) were assayed in individual macaques over the course of the experiment using the Mesoscale kit as described in Materials and Methods. Each symbol represents a specific animal throughout. Neutralizing antibody titers (c, f, i, and l) were measured using a lentiviral pseudovirus expressing the human SARS-CoV-2 spike as described in Materials and Methods. Values are reciprocal dilutions that produced an 80% reduction in pseudovirus infection (c, f, i, and l). Statistics comparing titers at days 7 dpi and 49 dpi were done using a two-way paired Student's *t* test. *, *P* < 0.05; ****, *P* < 0.0001. Unlabeled comparisons were not statistically significant. Analysis of differences between experimental groups was done by one-way ANOVA with a Dunnett's multiple comparisons posttest. The ability of sera from 28 dpi to neutralize live SARS-CoV-2 confirmed results from the pseudovirus neutralization assay (Fig. S4).

CD4-depleted animals (Fig. 1g). The binding and neutralizing antibody titers waned by 42 dpi but rapidly expanded upon reinfection regardless of T cell depletions. For example, the nAb titers in the CD4-depleted animals were all less than 100 at the time of reinfection, but all animals had strong anamnestic nAb responses and were strongly protected from disease. Thus, memory B cell responses were associated with protection.

Cervical lymph node analysis. T cell levels in blood may not reflect levels in tissues, where cells may be more refractory to antibody-mediated depletions. No biopsy specimens were taken during the course of the experiment, but immunohistochemical staining was used to examine CD4⁺ and CD8⁺ T cells in necropsy tissues at the termination of the experiment (56 dpi). A representative section from a cervical lymph node, which drains the upper respiratory tract, is shown for each experimental group (Fig. 5).

CD4⁺ T cells. Sections of cervical lymph nodes from controls showed abundant CD4⁺ T cells in periaarteriolar lymphoid sheaths and the mantle zone of lymphoid follicles. Representative low- and high-magnification sections are shown in Fig. 5a. In comparison, CD4⁺ T cells were greatly reduced in the lymphoid follicles from CD4-depleted animals, although not completely gone (Fig. 5b). CD4⁺ T cell staining appeared normal in the CD8-depleted animals (Fig. 5c), but the CD4/CD8-depleted animals showed moderately decreased staining (Fig. 5d). Immunohistochemical staining of spleen sections gave results very similar to those of the cervical lymph nodes (Fig. S4). These findings cannot distinguish between T cells that were never depleted and those that resulted from reseeding of the tissues over the 8 weeks of the experiment.

CD8⁺ T cells. Compared to the control (Fig. 5e), the CD8⁺ T cell staining in the CD4-depleted animals appeared normal or slightly increased (Fig. 5f). The lymph nodes from both the CD8-depleted and dually depleted animals showed dramatically reduced CD8⁺ T cell staining (Fig. 5g and h).

B cells. The lymph nodes were also stained with anti-CD20 to detect B cells. Unlike the diminished levels of B cells in the blood of CD4-depleted animals (Fig. 1g), no difference in total CD20 staining was observed in the lymph nodes (Fig. 5i to l).

DISCUSSION

It has been previously reported that rhesus macaques infected with SARS-CoV-2 are resistant to severe disease, similar to most young adult humans (13). In this study, we investigated the role of T cells in the natural resistance of macaques to severe COVID-19. The study could be relevant to human disease because HIV patients with CD4⁺ T cell counts below 350/ μ l are associated with an increased risk for severe COVID-19 (18). Furthermore, SARS-CoV-2 infections induce T cell lymphopenia and T cell dysfunction (5–12), and more severe lymphopenia is associated with more severe COVID-19 (19). The individual subset depletions in our study (Fig. 1) resulted in more severe T cell loss than has been reported in severe COVID-19 (19) and allowed us to analyze both CD4⁺ and CD8⁺ subsets independently. In neither of these studies did the individual subset depletions result in higher virus loads or more severe clinical signs. However, severe COVID-19 is associated with concurrent loss of both CD4⁺ and CD8⁺ T cells. When we depleted both T cell subsets in the macaques, the CD8⁺ T cell depletions in the blood were virtually complete (Fig. 1l), but only one animal had complete CD4⁺ T cell depletion (CD4/8-1), and the other five animals were not well depleted of CD4⁺ T cells (Fig. 1k). Although the well-depleted animal did not suffer higher virus loads or worse clinical signs, the fact that the other five animals were not strongly depleted of CD4⁺ T cells places a caveat on interpreting the results. Depletion of either CD4⁺ or CD8⁺ T cells only slightly prolonged the recovery of macaques from a first infection with SARS-CoV-2 and had little or no impact on recovery from reinfection. This is not to say that T cells do not normally play roles in controlling acute SARS-CoV-2 infections or anamnestic responses, but rather that such roles do not appear critical or that their loss may be compensated for by other immune cells in macaques. However, if new SARS-CoV-2 variants arise with mutant spike proteins that are poorly recognized by antibodies, T cell responses could become much more significant in the rational design of vaccines (20). On the other hand, we found no evidence that T cells played a pathological role in the development of disease in macaques, as the disease severity in the T cell-replete animals was similar to that in the T cell-depleted animals.

It was unexpected that the CD4-depleted animals would class switch to IgG during primary infection and mount anamnestic IgG responses upon second infection. The SARS-CoV-2 virion does not contain classic T cell-independent antigens, which are typically rigid

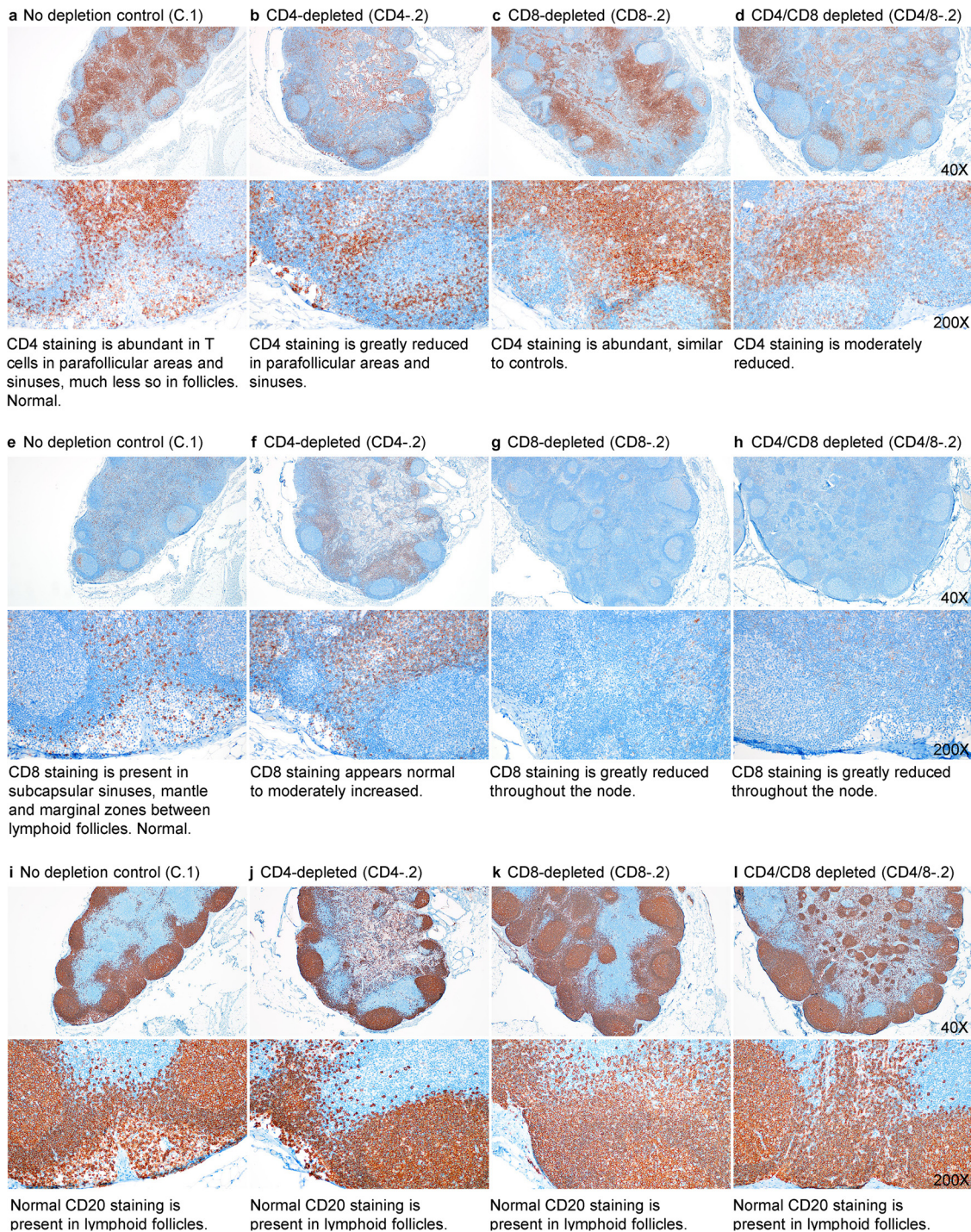


FIG 5 Immunohistochemical staining of cervical lymph nodes for CD4⁺ and CD8⁺ T cells and B cells. Representative animals from each experimental group are shown. (a to d) Cervical lymph nodes stained with anti-CD4 antibodies. (e to h) Cervical lymph nodes stained with anti-CD8 antibodies. (i to l) Cervical lymph nodes stained with anti-CD20 antibodies to detect B cells. None of the tissues stained positive for the presence of SARS-CoV-2 at 56 dpi.

arrays of 30 or more repeated epitopes optimally separated by 5 to 10 nm such as those present on vesicular stomatitis virus (21, 22). However, there is evidence that SARS-CoV-2 patients mount extrafollicular B cell responses (23, 24), a type of response that has been shown in mouse studies to produce IgM memory B cells and also IgG class-switched memory B cells in a T cell-independent manner (25, 26). In that regard, most of the mice in all of the groups in this study mounted anamnestic IgM responses (Fig. 4a, d, g, and j), and

most also produced inflammatory CXCL-10 (Fig. S5), a biomarker associated with severe COVID-19 in humans and also associated with extrafollicular B cells in COVID-19 patients (24). That said, our analysis did not definitively demonstrate the presence of extrafollicular B cells or T cells. We also cannot exclude the possibility that despite high-level T cell depletions in the blood (Fig. 1d), sufficient CD4⁺ T cells remained present in lymphoid tissues to generate immunological help. However, the diminished CD4 staining in cervical lymph nodes at 56 dpi (Fig. 5b), the absence of any observable CD4⁺ T cell responses in the blood in the weeks following infection (Fig. 1e) and the strongly ablated B cell responses observed in the blood of the CD4-depleted animals compared to controls (Fig. 1g) argue that the CD4 depletions had a major impact on the T cell repertoires of the animals. B cell activation and stimulation of proliferation typically occur in secondary lymphoid organs, where B cells interact with CD4⁺ T cells (27), but the B cells then disperse and appear in the blood at least transiently, as observed in the control animals but not the CD4-depleted animals (Fig. 1d). It is also possible that help for immunoglobulin class switching was provided by compensatory responses from non-CD4⁺ cells. For example, in the absence of CD4⁺ T cells, mouse studies with inactivated influenza virus revealed that CD4⁻ CD8⁻ $\alpha\beta$ T cells could provide help for immunoglobulin class switching (28). In addition, interferon gamma-producing $\gamma\delta$ T cells have also been shown to enable compensatory immunoglobulin class switching (29).

In the work of McMahan et al. (17), rhesus macaques previously infected with SARS-CoV-2 were depleted of CD8⁺ T cells prior to reinfection, which occurred at 7 weeks after the first infection. In that case, all 5 of the depleted animals showed breakthrough virus in nasal swabs, whereas only one of the controls did. This finding led to the conclusion that CD8⁺ T cell depletion abrogated the recovery of convalescent macaques. Our study found a slightly prolonged recovery from the first infection but not from reinfection due to CD8⁺ T cell depletion. In our experiments, which employed the same Washington virus isolate (identical sequences) and depleting antibody, half of the control animals and half of the CD8-depleted animals showed breakthrough virus in nasal swabs following reinfection, as measured by sgRNA (Fig. 2). Experimental differences included the timing of the rechallenge and the CD8 depletions. While we found less effect on reinfection than the study by McMahan et al. (17), the difference between these two small studies is not statistically different. Both our studies indicate a role for CD8⁺ T cells but a more important role for virus-specific antibodies. It would be of interest in further studies to determine whether T cell immunity in the absence of antibody responses would be sufficient for protection.

Old age in humans plays a significant role in susceptibility to severe disease and death from SARS-CoV-2 infections, and it is well known that advanced age is associated with age-related degradation of the immune system (immunosenescence) (30) and dysregulated inflammatory responses (inflammaging) (31), which result in increased vulnerability to infectious diseases. Thus, aged individuals are likely to be considerably less able than adult macaques to compensate for immune deficiencies such as SARS-CoV-2-induced lymphopenia. The oldest macaque in our study was 9 years old, which is not considered aged. It has been shown that aged macaques develop lower antibody responses to SARS-CoV-2 infections (32, 33), so it is possible that different results would have been obtained with aged macaques. That said, our results from adult macaques with profound depletion of either CD4⁺ or CD8⁺ T cells leads to the conclusion that neither subset played a critical role in recovery from acute disease or reinfection. On the other hand, anamnestic antibody responses were strongly associated with recovery from a second infection and reduced disease.

The current study did not address the requirement for T cells in long-term memory and protection from COVID-19, which will require further experiments. We are currently faced with the emergence of multiple SARS-CoV-2 variants containing mutations in RBD that allow partial or total escape from monoclonal antibodies and reduce vaccine-induced virus neutralization by antibodies (34, 35). Furthermore, vaccines based on the original spike sequence appear less protective against the new variants,

particularly the South African B.1.351 variant. It is not known whether emerging variants are also evolving to escape T cell responses, but the current results suggest that there may be less evolutionary pressure to escape T cell responses than B cell/antibody responses. As a final note, while the rhesus macaque is considered the gold standard model for mild COVID-19, there may be aspects of the human disease that are not well recapitulated. Our results do not preclude lymphopenia as a contributory factor in severe COVID-19 in humans but rather suggest that other contributory factors are likely involved and that further investigations should focus on them as well.

MATERIALS AND METHODS

Ethics and biosafety statement. All *in vivo* experiments were performed in accordance with Animal Study Proposal RML 2020-046-E approved by the Institutional Animal Care and Use Committee of Rocky Mountain Laboratories (National Institutes of Health [NIH]) and carried out by certified staff in an Association for Assessment and Accreditation of Laboratory Animal Care International-accredited facility, according to the institution's guidelines for animal use, following the guidelines and basic principles in the NIH *Guide for the Care and Use of Laboratory Animals* (36), the Animal Welfare Act, and the United States Department of Agriculture and the United States Public Health Service Policy on Humane Care and Use of Laboratory Animals. Rhesus macaques were housed in adjacent individual primate cages allowing social interactions, in a climate-controlled room with a fixed light/dark cycle (12 h light/12 h dark). Commercial monkey chow, treats, and fruit were provided twice daily by trained personnel. Water was available *ad libitum*. Environmental enrichment consisted of a variety of human interaction, manipulanda, commercial toys, videos, and music. The Institutional Biosafety Committee (IBC) approved work with infectious SARS-CoV-2 strains under biosafety level 3 (BSL-3) conditions. Sample inactivation was performed according to IBC-approved standard operating procedures for removal of specimens from high containment.

Animals. In the first experiment, 12 adult male rhesus macaques aged 2 1/2 to 5 years were randomly divided into four groups of three. All animals were euthanized and necropsied on day 56 (day 14 after re-exposure). The experiment was repeated with a second group of 12 rhesus macaques, including 10 females aged 3 to 10 years old and 2 males aged 4 and 5 years old.

T cell depletions. At day -7 (relative to infection), the animals were anesthetized and underwent clinical exams. Also at day -7, according to group assignment, the macaques received a one-time subcutaneous injection (10 mg/kg) of either (i) rhesus recombinant anti-CD4 depleting antibody (CD4R1), (ii) a mouse/rhesus CDR-grafted form of the depleting anti-CD8 α antibody M-T807 (each at 10 mg/ml prepared in pharmaceutical grade by the NIH Nonhuman Primate Reagent Resource), (iii) both CD4R1 and M-T807, or (iv) physiological saline. At days -4, 0, and +3, the animals received 5-mg/kg intravenous (i.v.) injections of the same antibodies (as per the provider's instructions).

Virus challenges. On days 0 and 42, the animals were anesthetized and inoculated with SARS-CoV-2 by four routes as previously described (13): intratracheal (4 ml), intranasal (0.5 ml in each nostril), oral (1 ml), and ocular (0.25 ml in each eye). Back titrations for the inocula showed titers of 3.16×10^5 50% tissue culture infectious doses (TCID₅₀)/ml for the first challenge of the first experiment, 4.3×10^5 TCID₅₀/ml for the second challenge, 4.4×10^5 TCID₅₀/ml for the first challenge of the second experiment and 4.3×10^5 TCID₅₀/ml for the second challenge of the second experiment. SARS-CoV-2 isolate nCoV-WA1-2020 (MN985325.1) (Vero passage 3) was provided by the Centers for Disease Control and Prevention and propagated as previously described (13). The virus stock used was fully sequenced (13) and found to be 100% identical to the initially deposited GenBank sequence (MN985325.1).

Clinical exams and necropsy. Macaques were monitored for clinical signs at least twice daily throughout the experiment using a standardized scoring sheet as previously described (13). On exam days (Fig. 1a), clinical parameters such as body weight, body temperature, and respiration rate were collected, as well as ventrodorsal and lateral chest radiographs. Chest radiographs were interpreted in a blind manner by a board-certified clinical veterinarian. The total white blood cell, lymphocyte, neutrophil, platelet, reticulocyte and red blood cell counts and hemoglobin and hematocrit values were determined from EDTA-treated blood using an IDEXX ProCyte DX Analyzer (IDEXX Laboratories). Necropsies were performed after euthanasia, and gross pathology was scored in a blind manner by a board-certified veterinary pathologist. Histopathological analysis of tissue slides was performed by a board-certified veterinary pathologist who was blind to the group assignment of the macaques.

Histology and immunohistochemistry. Tissues were fixed in 10% neutral buffered formalin with two changes, for a minimum of 7 days according to IBC-approved standard operating procedures (SOP). Tissues were processed with a Sakura VIP-6 Tissue Tek, on a 12-h automated schedule, using a graded series of ethanol, xylene, and PureAffin. Embedded tissues were sectioned at 5 μ m and dried overnight at 42°C prior to staining with hematoxylin and eosin. Specific staining was detected using SARS-CoV/SARS-CoV-2 nucleocapsid antibody (Sino Biological cat#40143-MM05) at a 1:1,000 dilution, CD4 antibody (Abcam catalog no. ab133616) at a 1:100 dilution, CD8 antibody (Sino Biological catalog no. 10980-T24) at a 1:500 dilution, and CD20 (Thermo Scientific catalog no. RB-9013) at a 1:250 dilution. The tissues were processed for immunohistochemistry using the Discovery Ultra automated stainer (Ventana Medical Systems) with a ChromoMap DAB kit (Roche Tissue Diagnostics catalog no. 760-159).

Morphometric analysis. CD4 and CD8 immunohistochemistry (IHC)-stained sections were scanned with an Aperio ScanScope XT (Aperio Technologies, Inc., Vista, CA) and analyzed using the ImageScope

Positive Pixel Count algorithm (version 9.1). The default parameters of the Positive Pixel Count (hue of 0.1 and width of 0.5) detected antigen adequately.

Thoracic radiographs. Ventrodorsal and right/left lateral radiographs were taken on clinical exam days prior to any other procedures. Radiographs were evaluated and scored for the presence of pulmonary infiltrates by two board-certified clinical veterinarians according to a standard scoring system (37). Briefly, each lung lobe was scored individually based on the following criteria: 0, normal examination; 1, mild interstitial pulmonary infiltrates; 2, moderate interstitial pulmonary infiltrates, perhaps with partial cardiac border effacement and small areas of pulmonary consolidation (alveolar patterns and air bronchograms); and 3, pulmonary consolidation as the primary lung pathology, seen as a progression from grade 2 lung pathology. Day 0 and 42 radiographs were taken prior to inoculation and thus serve as a baseline for each animal. As such, scores for all lung lobes on day 0 were set to 0 (normal examination). All subsequent radiographs were compared to the day 0 radiographs, evaluated for changes from baseline, and scored based on the criteria noted above. At study completion, thoracic radiograph findings are reported as a single radiograph score for each animal on each exam day. To obtain this score, the scores assigned to each of the six lung lobes are added together and recorded as the radiograph score for each animal on each exam day. Scores therefore range from 0 to 18 for each animal on each exam day.

Spike- and RBD-binding IgM and IgG. IgM and IgG titers were quantified from serum collected for all animals on days 0, 7, 14, 28, 42, and 49. A Meso Scale Discovery V-PLEX SARS-CoV-2 panel 1 kit (Rockville, MD) was used for determining antibody binding for IgG (K15359U) and IgM (K15360U) specific for SARS-CoV-2 S1 RBD. Protocols were followed as per the manufacturer's recommendations. All diluted samples fell within standard curve ranges. A Meso Scale Discovery MESO QuickPlex SQ 120 instrument was used for measuring chemiluminescence with Methodical Minds acquisition software. Analysis was performed on the Discovery Workbench software (version 4.0). Concentrations are relative to internal controls and were reported as arbitrary units (AU) per milliliter. GraphPad Prism 8 was used for preparation of graphs and statistical analysis.

Virus-neutralizing antibody assay. Neutralizing-antibody titers were determined in plasma samples using a modified lentivirus-based pseudovirus assay (38). Plasmids encoding an Env-defective HIV-1 backbone tagged with the nanoluciferase gene (HIV-1_{NL}Δ Env-NanoLuc) and an expression construct for the SARS-CoV-2 spike lacking 19 amino acids of the cytoplasmic tail encoding the endoplasmic reticulum (ER) retention motif (CMV-SARS-CoV-2 SΔ19) were kind gifts from Paul Bieniasz (Rockefeller University). Pseudovirions were prepared in HEK293T cells by cotransfecting 60 μg of HIV-1_{NL}Δ Env-NanoLuc and CMV-SARS-CoV-2 SΔ19 at a 3:2 ratio in T-175 flasks using the calcium phosphate method and then were concentrated by ultracentrifugation in a sucrose cushion (39). We utilized A549-ACE2 cells (40) as target cells, as these cells attached better to the culture plate than 293T-ACE2 cells (38), allowing extensive washes given that the nanoluciferase reporter yielded high backgrounds. A549-ACE2 cells were cultured in complete medium containing F-12 Ham's medium (Corning), 10% fetal bovine serum (Atlanta Biologicals), and 1% penicillin-streptomycin-glutamine (Corning).

For the nAb assay, a previously determined titer (300,000 to 400,000 relative light units [RLU] per well) of pseudovirus was cocubated with serial 5-fold dilutions of plasma (1:5 to 1:15,625) in 100 μl complete medium at 37°C for 1 h in 96-well round-bottom plates. In duplicate, 40 μl of the virus-plasma mixture was combined with 160 μl of complete medium containing 10,000 A549-ACE2 cells. The virus-plasma-cell mixtures were plated in white polystyrene plates (Millipore-Sigma) and cultured at 37°C in 5% CO₂. After 48 h, the spent medium in each well was removed, and the cells were washed four times with 200 μl phosphate-buffered saline (PBS). After the last wash, 100 μl of PBS was dispensed into each well, and mixed with 100 μl of Nano-Glo luciferase substrate working solution (Promega). RLU values were measured in a VictorX5 luminometer (Perkin Elmer). To compute 80% inhibitory concentrations (IC₈₀), the mean RLUs of virus-only wells ($n=6$) in each plate were set as 100% infection. Duplicate RLUs for each plasma dilution were averaged and normalized against virus-only wells. Best-fit nonlinear regression curves were constructed based on a two-phase decay equation (GraphPad Prism 8), and 80% inhibition values (20% infection) were interpolated. nAb titers were reported as reciprocal plasma dilutions.

Titers of nAb against live virus were also determined for a subset of plasma samples (28 dpi) in A549-ACE2 cells in a 48-well plate format (40). Briefly, 1:20, 1:100, and 1:500 dilutions of plasma were cocubated at 37°C for 1 h with a nonsaturating dose of the SARS-CoV-2 USA-WA1/2020 strain that would yield ~100,000 copies in the quantitative PCR assay. After 24 h, virus copy numbers were evaluated from culture supernatant using nucleocapsid-specific primers and probes as we previously described (40).

Virus detection. RNA was extracted from swabs and bronchoalveolar lavage specimens using the QIAamp viral RNA kit (Qiagen) according to the manufacturer's instructions and as described elsewhere (13). Five microliters of RNA was used in a one-step real-time reverse transcription-PCR (RT-PCR) E assay using the Rotor-Gene probe kit (Qiagen) according to instructions of the manufacturer. In each run, standard dilutions of counted RNA standards were run in parallel, to calculate copy numbers in the samples. For detection of SARS-CoV-2 mRNA, primers targeting open reading frame 7 (ORF7) were designed as follows: forward primer, 5'-TCCCAGGTAACAAACCAACC-3'; reverse primer, 5'-GCTCACAAGTAGCGAGTGTTAT-3'; and probe, 6-carboxyfluorescein (FAM)-ZEN-CTTGTAGATCTGTTCTCTAAACGAAC-3'-Iowa black fluorescent quencher (IBFQ). Five microliters of RNA was used in a one-step real-time RT-PCR using the Rotor-Gene probe kit (Qiagen) according to instructions of the manufacturer. In each run, standard dilutions of counted RNA standards were run in parallel, to calculate copy numbers in the samples. Detection of viral E gene subgenomic mRNA (sgRNA) was performed using RT-PCR as described elsewhere (15). The forward primer

(5'–3') was CGATCTCTGTAGATCTGTTCTC, the reverse primer was ATATTGCAGCAGTACGCACACA, and the probe was FAM-ACACTAGCCATCCTTACTGCGCTTCG-ZEN-Iowa black hole quencher (IBHQ).

Flow cytometry. Immune cell marker analysis was performed on freshly isolated PBMCs following enrichment after a standard Histopaque 1077 (Sigma) centrifugation procedure in 15-ml Leucosep tubes (Greiner Bio-One) from EDTA blood samples. Briefly, 3 ml of room temperature Histopaque 1077 was added to Leucosep tubes and centrifuged at $1,000 \times g$ for 1 min. Blood was diluted 1:2 in $1 \times$ Dulbecco's PBS (DPBS), transferred into the Leucosep tube, and centrifuged at $1,000 \times g$ for 10 min at room temperature without the brake. The enriched live PBMC fraction was collected, washed in $1 \times$ DPBS, and then transferred to plates for staining. Cells were incubated for 30 min with the following cell surface antibodies: BUV661–anti-CD45 (D058-128; BD Biosciences 741657, lot 0198214), phycoerythrin (PE)-Cy7–anti-CD20 (2H7; BD Biosciences 560735, lot 0170481), BV786–anti-CD3 (SP34-2; BD Biosciences 563918, lot 0133645), fluorescein isothiocyanate (FITC)–anti-CD8 (DK25, Millipore FCMAB176F, lot 3398058), and Pacific Blue–anti-CD4 (OKT4; BioLegend 317424, lot B258189) in 2% FBS–PBS supplemented with brilliant stain buffer (BD Biosciences). Intracellular staining was performed using the Foxp3 transcription factor staining buffer set (Thermo Fisher) following the company's recommendation. Cells were incubated for 30 min with the following antibodies: PE-anti-Foxp3 (259D; BioLegend 3202080, lot B293618) and AF700-anti-Ki-67 (B56; BD Biosciences 561277, lot 9315354). Live lymphocytes were gated by a side scatter area (SSC-A) and a forward scatter area (FSC-A) gate, by forward scatter height (FSC-H) and FSC-A to exclude doublets, and then by time to exclude artifacts caused by erratic sample flow. Gating strategies for B cells and CD8⁺ and CD4⁺ T cells are shown in Fig. S4. The multiparameter data were collected in a BSL-4 facility using a Cytoflex LX flow cytometer (Beckman Coulter) and analyzed using FlowJo software (version 10.7.1; TreeStar, Inc.).

Cytokine analysis. Cytokines and growth factors were analyzed from blood collected for all animals on days 0, 1, 3, 7, 42, 43, 45, and 49, and BAL fluid was collected for all animals on days 1, 7, 43, 49, and 56. An NHP XL cytokine Luminex Performance kit (R&D Systems catalog no. FCSTM21) was used according to manufacturer's recommendations to determine the levels of the following analytes: CCL2, IP-10, granulocyte colony-stimulating factor (G-CSF), alpha interferon (IFN- α), IFN- β , IFN- γ , interleukin 1 β (IL-1 β), IL-6, and tumor necrosis factor alpha (TNF- α). A Bio-plex 200 Luminex system (Bio-Rad) was used to read and analyze the samples. Concentrations are reported in picograms per milliliter. GraphPad Prism 8 was used for preparation of graphs and statistical analysis.

Statistical analyses. All statistics were analyzed using Prism Mac OS version 8.4.3 software. The specific tests used for statistical analyses are listed in the figure legends. The *P* value cutoff for statistical significance was set to 0.05. *P* values are shown in the figures or figure legends.

Data availability. Underlying data sets for Fig. 1 and 4 have been deposited to Figshare (https://figshare.com/articles/dataset/Recovery_from_acute_SARS-CoV-2_infection_and_development_of_anamnestic_immune_responses_in_T_cell-depleted_rhesus_macaques/14403557).

SUPPLEMENTAL MATERIAL

Supplemental material is available online only.

FIG S1, JPG file, 1.1 MB.

FIG S2, JPG file, 1.6 MB.

FIG S3, TIF file, 0.3 MB.

FIG S4, TIF file, 0.2 MB.

TABLE S1, DOCX file, 0.02 MB.

ACKNOWLEDGMENTS

This work was supported by the Intramural Research Program of the National Institute of Allergy and Infectious Diseases of the National Institutes of Health and by Institutional funds from the Division of Infectious Diseases, University of Colorado AMC (M.L.S.). Depleting antibodies were obtained from the Nonhuman Primate Reagent Resource.

Many thanks go to the Rocky Mountain Labs Veterinary Branch animal caretakers for all their hard work. Thanks go to Dan Long for his input on the histology and to Emmie de Wit and Vincent Munster for advice and consultation. Thanks go to Leonard Evans for review of the manuscript.

K.J.H. contributed to experimental concept, design, data analysis and interpretation, figure preparation, and statistical analyses and wrote the paper. H.F. contributed to experimental design, supervision of animal experiments, interpretation of results and manuscript revision. F.F. contributed to experimental design and scheduling, performed *in vivo* and *in vitro* experiments, animal scoring, collection and preparation of experimental samples, and performed necropsies. D.R. performed viral analyses, cytokine analyses, figure preparation and interpretation of results. R.J.M. performed viral analyses. L.M. designed and performed flow cytometry experiments and analyses and prepared figures. M.L.S., K.G., B.S.B.,

and K.L.M. designed and performed neutralizing-antibody assays interpreted results and prepared figures. M.M.C. analyzed plasma for virus-specific antibodies and performed viral analyses. A.C. collected and prepared samples and designed and performed flow cytometry experiments. A.O., J.L., and K.M.-W. performed animal experiments and collected and prepared samples. C.S. performed necropsies and histological analyses. R.R. performed immunohistochemical analyses. P.H. contributed to scheduling experiments and performed clinical exams, necropsies, bloodwork and radiographs. B.S. performed clinical exams, necropsies, bloodwork, and radiographs. N.V.D. contributed to experimental design. C.C. performed necropsies. G.S. performed necropsies. W.L.S. contributed to scheduling and logistics. D.W.H. contributed to experimental design.

We declare no competing interests.

REFERENCES

- Koblischke M, Traugott MT, Medits I, Spitzer FS, Zoufaly A, Weseslindtner L, Simonitsch C, Seitz T, Hoepfer W, Puchhammer-Stockl E, Aberle SW, Fodinger M, Bergthaler A, Kundi M, Heinz FX, Stiasny K, Aberle JH. 2020. Dynamics of CD4 T cell and antibody responses in COVID-19 patients with different disease severity. *Front Med (Lausanne)* 7:592629. <https://doi.org/10.3389/fmed.2020.592629>.
- Chen Z, John Wherry E. 2020. T cell responses in patients with COVID-19. *Nat Rev Immunol* 20:529–536. <https://doi.org/10.1038/s41577-020-0402-6>.
- Grifoni A, Weiskopf D, Ramirez SI, Mateus J, Dan JM, Moderbacher CR, Rawlings SA, Sutherland A, Premkumar L, Jadi RS, Marrama D, de Silva AM, Frazier A, Carlin AF, Greenbaum JA, Peters B, Krammer F, Smith DM, Crotty S, Sette A. 2020. Targets of T cell responses to SARS-CoV-2 coronavirus in humans with COVID-19 disease and unexposed individuals. *Cell* 181:1489–1501.E15. <https://doi.org/10.1016/j.cell.2020.05.015>.
- Ni L, Ye F, Cheng ML, Feng Y, Deng YQ, Zhao H, Wei P, Ge J, Gou M, Li X, Sun L, Cao T, Wang P, Zhou C, Zhang R, Liang P, Guo H, Wang X, Qin CF, Chen F, Dong C. 2020. Detection of SARS-CoV-2-specific humoral and cellular immunity in COVID-19 convalescent individuals. *Immunity* 52:971–977.E3. <https://doi.org/10.1016/j.immuni.2020.04.023>.
- Diao B, Wang C, Tan Y, Chen X, Liu Y, Ning L, Chen L, Li M, Liu Y, Wang G, Yuan Z, Feng Z, Zhang Y, Wu Y, Chen Y. 2020. Reduction and functional exhaustion of T cells in patients with coronavirus disease 2019 (COVID-19). *Front Immunol* 11:827. <https://doi.org/10.3389/fimmu.2020.00827>.
- Giamarellos-Bourboulis EJ, Netea MG, Rovina N, Akinosoglou K, Antoniadou A, Antonakos N, Damoraki G, Gkavogianni T, Adami ME, Katsaounou P, Ntaganou M, Kyriakopoulou M, Dimopoulos G, Koutsodimitropoulos I, Velissaris D, Koufargyris P, Karageorgos A, Katrini K, Lekakis V, Lupse M, Kotsaki A, Renieris G, Theodoulou D, Panou V, Koukaki E, Koulouris N, Gogos C, Koutsoukou A. 2020. Complex immune dysregulation in COVID-19 patients with severe respiratory failure. *Cell Host Microbe* 27:992–1000.E3. <https://doi.org/10.1016/j.chom.2020.04.009>.
- Song CY, Xu J, He JQ, Lu YQ. 2020. Immune dysfunction following COVID-19, especially in severe patients. *Sci Rep* 10:15838. <https://doi.org/10.1038/s41598-020-72718-9>.
- Kusnadi A, Ramirez-Suastegui C, Fajardo V, Chee SJ, Meckiff BJ, Simon H, Pelosi E, Seumois G, Ay F, Vijayanand P, Ottensmeier CH. 2021. Severely ill COVID-19 patients display impaired exhaustion features in SARS-CoV-2-reactive CD8+ T cells. *Sci Immunol* 6:eabe4782. <https://doi.org/10.1126/sciimmunol.abe4782>.
- Westmeier J, Paniskaki K, Karakose Z, Werner T, Sutter K, Dolff S, Overbeck M, Limmer A, Liu J, Zheng X, Brenner T, Berger MM, Witzke O, Trilling M, Lu M, Yang D, Babel N, Westhoff T, Dittmer U, Zelinsky G. 2020. Impaired cytotoxic CD8(+) T cell response in elderly COVID-19 patients. *mBio* 11:e02243-20. <https://doi.org/10.1128/mBio.02243-20>.
- Liu J, Li H, Luo M, Liu J, Wu L, Lin X, Li R, Wang Z, Zhong H, Zheng W, Zhou Y, Jiang D, Tan X, Zhou Z, Peng H, Zhang G. 2020. Lymphopenia predicted illness severity and recovery in patients with COVID-19: a single-center, retrospective study. *PLoS One* 15:e0241659. <https://doi.org/10.1371/journal.pone.0241659>.
- Tan L, Wang Q, Zhang D, Ding J, Huang Q, Tang YQ, Wang Q, Miao H. 2020. Lymphopenia predicts disease severity of COVID-19: a descriptive and predictive study. *Signal Transduct Target Ther* 5:33. <https://doi.org/10.1038/s41392-020-0148-4>.
- Zhao Q, Meng M, Kumar R, Wu Y, Huang J, Deng Y, Weng Z, Yang L. 2020. Lymphopenia is associated with severe coronavirus disease 2019 (COVID-19) infections: a systemic review and meta-analysis. *Int J Infect Dis* 96:131–135. <https://doi.org/10.1016/j.ijid.2020.04.086>.
- Munster VJ, Feldmann F, Williamson BN, van Doremalen N, Perez-Perez L, Schulz J, Meade-White K, Okumura A, Callison J, Brumbaugh B, Avanzato VA, Rosenke R, Hanley PW, Saturday G, Scott D, Fischer ER, de Wit E. 2020. Respiratory disease in rhesus macaques inoculated with SARS-CoV-2. *Nature* 585:268–272. <https://doi.org/10.1038/s41586-020-2324-7>.
- Williamson BN, Feldmann F, Schwarz B, Meade-White K, Porter DP, Schulz J, van Doremalen N, Leighton I, Yinda CK, Perez-Perez L, Okumura A, Lovaglio J, Hanley PW, Saturday G, Bosio CM, Anzick S, Barbian K, Cihlar T, Martens C, Scott DP, Munster VJ, de Wit E. 2020. Clinical benefit of remdesivir in rhesus macaques infected with SARS-CoV-2. *Nature* 585:273–276. <https://doi.org/10.1038/s41586-020-2423-5>.
- Chandrashekar A, Liu J, Martinot AJ, McMahan K, Mercado NB, Peter L, Tostanoski LH, Yu J, Maliga Z, Nekorchuk M, Busman-Sahay K, Terry M, Wrijil LM, Ducat S, Martinez DR, Atyeo C, Fischinger S, Burke JS, Slein MD, Pessaint L, Van Ry A, Greenhouse J, Taylor T, Blade K, Cook A, Finneyfrock B, Brown R, Teow E, Velasco J, Zahn R, Wegmann F, Abbink P, Bondzie EA, Dagotto G, Gebre MS, He X, Jacob-Dolan C, Kordana N, Li Z, Lifton MA, Mahrokhanian SH, Maxfield LF, Nityanandam R, Nkolola JP, Schmidt AG, Miller AD, Baric RS, Alter G, Sorger PK, Estes JD, et al. 2020. SARS-CoV-2 infection protects against rechallenge in rhesus macaques. *Science* 369:812–817. <https://doi.org/10.1126/science.abc4776>.
- Deng W, Bao L, Liu J, Xiao C, Liu J, Xue J, Lv Q, Qi F, Gao H, Yu P, Xu Y, Qu Y, Li F, Xiang Z, Yu H, Gong S, Liu M, Wang G, Wang S, Song Z, Liu Y, Zhao W, Han Y, Zhao L, Liu X, Wei Q, Qin C. 2020. Primary exposure to SARS-CoV-2 protects against reinfection in rhesus macaques. *Science* 369:818–823. <https://doi.org/10.1126/science.abc5343>.
- McMahan K, Yu J, Mercado NB, Loos C, Tostanoski LH, Chandrashekar A, Liu J, Peter L, Atyeo C, Zhu A, Bondzie EA, Dagotto G, Gebre MS, Jacob-Dolan C, Li Z, Nampanya F, Patel S, Pessaint L, Van Ry A, Blade K, Yalley-Ogunro J, Cabus M, Brown R, Cook A, Teow E, Andersen H, Lewis MG, Lauffenburger DA, Alter G, Barouch DH. 2021. Correlates of protection against SARS-CoV-2 in rhesus macaques. *Nature* 590:630–634. <https://doi.org/10.1038/s41586-020-03041-6>.
- Hoffmann C, Casado JL, Harter G, Vizcarra P, Moreno A, Cattaneo D, Meraviglia P, Spinner CD, Schabaz F, Grunwald S, Gervasoni C. 2021. Immune deficiency is a risk factor for severe COVID-19 in people living with HIV. *HIV Med* 22:372–378. <https://doi.org/10.1111/hiv.13037>.
- Zhang H, Wu T. 2020. CD4+T, CD8+T counts and severe COVID-19: a meta-analysis. *J Infect* 81:e82–e84. <https://doi.org/10.1016/j.jinf.2020.06.036>.
- Burton DR, Walker LM. 2020. Rational vaccine design in the time of COVID-19. *Cell Host Microbe* 27:695–698. <https://doi.org/10.1016/j.chom.2020.04.022>.
- Karrer U, Lopez-Macias C, Oxenius A, Odermatt B, Bachmann MF, Kalinke U, Bluethmann H, Hengartner H, Zinkernagel RM. 2000. Antiviral B cell memory in the absence of mature follicular dendritic cell networks and classical germinal centers in TNFR1-/- mice. *J Immunol* 164:768–778. <https://doi.org/10.4049/jimmunol.164.2.768>.
- Hangartner L, Zinkernagel RM, Hengartner H. 2006. Antiviral antibody responses: the two extremes of a wide spectrum. *Nat Rev Immunol* 6:231–243. <https://doi.org/10.1038/nri1783>.
- Newell KL, Clemmer DC, Cox JB, Kayode YI, Zoccoli-Rodriguez V, Taylor HE, Endy TP, Wilmore JR, Winslow GM. 2021. Switched and unswitched

- memory B cells detected during SARS-CoV-2 convalescence correlate with limited symptom duration. *PLoS One* 16:e0244855. <https://doi.org/10.1371/journal.pone.0244855>.
24. Woodruff MC, Ramonell RP, Nguyen DC, Cashman KS, Saini AS, Haddad NS, Ley AM, Kyu S, Howell JC, Ozturk T, Lee S, Suryadevara N, Case JB, Bugrovsky R, Chen W, Estrada J, Morrison-Porter A, Derrico A, Anam FA, Sharma M, Wu HM, Le SN, Jenks SA, Tipton CM, Staitieh B, Daiss JL, Ghosn E, Diamond MS, Carnahan RH, Crowe JE, Jr, Hu WT, Lee FE, Sanz I. 2020. Extrafollicular B cell responses correlate with neutralizing antibodies and morbidity in COVID-19. *Nat Immunol* 21:1506–1516. <https://doi.org/10.1038/s41590-020-00814-z>.
 25. Allman D, Wilmore JR, Gaudette BT. 2019. The continuing story of T-cell independent antibodies. *Immunol Rev* 288:128–135. <https://doi.org/10.1111/imr.12754>.
 26. Di Niro R, Lee SJ, Vander Heiden JA, Elsner RA, Trivedi N, Bannock JM, Gupta NT, Kleinstein SH, Vigneault F, Gilbert TJ, Meffre E, McSorley SJ, Shlomchik MJ. 2015. Salmonella infection drives promiscuous B cell activation followed by extrafollicular affinity maturation. *Immunity* 43:120–131. <https://doi.org/10.1016/j.immuni.2015.06.013>.
 27. Akkaya M, Kwak K, Pierce SK. 2020. B cell memory: building two walls of protection against pathogens. *Nat Rev Immunol* 20:229–238. <https://doi.org/10.1038/s41577-019-0244-2>.
 28. Sha Z, Compans RW. 2000. Induction of CD4(+) T-cell-independent immunoglobulin responses by inactivated influenza virus. *J Virol* 74:4999–5005. <https://doi.org/10.1128/jvi.74.11.4999-5005.2000>.
 29. Maloy KJ, Odermatt B, Hengartner H, Zinkernagel RM. 1998. Interferon gamma-producing gammadelta T cell-dependent antibody isotype switching in the absence of germinal center formation during virus infection. *Proc Natl Acad Sci U S A* 95:1160–1165. <https://doi.org/10.1073/pnas.95.3.1160>.
 30. Aiello A, Farzaneh F, Candore G, Caruso C, Davinelli S, Gambino CM, Ligotti ME, Zareian N, Accardi G. 2019. Immunosenescence and its hallmarks: how to oppose aging strategically? A review of potential options for therapeutic intervention. *Front Immunol* 10:2247. <https://doi.org/10.3389/fimmu.2019.02247>.
 31. Frasca D, Blomberg BB. 2016. Inflammaging decreases adaptive and innate immune responses in mice and humans. *Biogerontology* 17:7–19. <https://doi.org/10.1007/s10522-015-9578-8>.
 32. Singh DK, Singh B, Ganatra SR, Gazi M, Cole J, Thippeshappa R, Alfson KJ, Clemmons E, Gonzalez O, Escobedo R, Lee TH, Chatterjee A, Goetz-Gazi Y, Sharan R, Gough M, Alvarez C, Blakley A, Ferdin J, Bartley C, Staples H, Parodi L, Callery J, Mannino A, Klaffke B, Escareno P, Platt RN, 2nd, Hodara V, Scordo J, Gautam S, Vilanova AG, Olmo-Fontanez A, Schami A, Oyejide A, Ajithdoss DK, Copin R, Baum A, Kyratsous C, Alvarez X, Ahmed M, Rosa B, Goodroe A, Dutton J, Hall-Urson S, Frost PA, Voges AK, Ross CN, Sayers K, Chen C, Hallam C, Khader SA, et al. 2021. Responses to acute infection with SARS-CoV-2 in the lungs of rhesus macaques, baboons and marmosets. *Nat Microbiol* 6:73–86. <https://doi.org/10.1038/s41564-020-00841-4>.
 33. Yu P, Qi F, Xu Y, Li F, Liu P, Liu J, Bao L, Deng W, Gao H, Xiang Z, Xiao C, Lv Q, Gong S, Liu J, Song Z, Qu Y, Xue J, Wei Q, Liu M, Wang G, Wang S, Yu H, Liu X, Huang B, Wang W, Zhao L, Wang H, Ye F, Zhou W, Zhen W, Han J, Wu G, Jin Q, Wang J, Tan W, Qin C. 2020. Age-related rhesus macaque models of COVID-19. *Animal Model Exp Med* 3:93–97. <https://doi.org/10.1002/ame2.12108>.
 34. Wang Z, Schmidt F, Weisblum Y, Muecksch F, Barnes CO, Finkin S, Schaefer-Babajew D, Cipolla M, Gaebler C, Lieberman JA, Yang Z, Abernathy ME, Huey-Tubman KE, Hurlley A, Turroja M, West KA, Gordon K, Millard KG, Ramos V, Da Silva J, Xu J, Colbert RA, Patel R, Dizon J, Unson-O'Brien C, Shimeliovich I, Gazumyan A, Caskey M, Bjorkman PJ, Casellas R, Hatzioannou T, Bieniasz PD, Nussenzweig MC. 2021. mRNA vaccine-elicited antibodies to SARS-CoV-2 and circulating variants. *bioRxiv* <https://doi.org/10.1101/2021.01.15.426911>.
 35. Wang P, Nair MS, Liu L, Iketani S, Luo Y, Guo Y, Wang M, Yu J, Zhang B, Kwong PD, Graham BS, Mascola JR, Chang JY, Yin MT, Sobieszczyk M, Kyratsous CA, Shapiro L, Sheng Z, Huang Y, Ho DD. 2021. Antibody resistance of SARS-CoV-2 variants B.1.351 and B.1.1.7. *Nature* 593:130–135. <https://doi.org/10.1038/s41586-021-03398-2>.
 36. National Research Council. 2011. Guide for the care and use of laboratory animals, 8th ed. National Academies Press, Washington, DC.
 37. Brining DL, Mattoon JS, Kercher L, LaCasse RA, Safronetz D, Feldmann H, Parnell MJ. 2010. Thoracic radiography as a refinement methodology for the study of H1N1 influenza in cynomolgus macaques (*Macaca fascicularis*). *Comp Med* 60:389–395.
 38. Schmidt F, Weisblum Y, Muecksch F, Hoffmann HH, Michailidis E, Lorenzi JCC, Mendoza P, Rutkowska M, Bednarski E, Gaebler C, Agudelo M, Cho A, Wang Z, Gazumyan A, Cipolla M, Caskey M, Robbiani DF, Nussenzweig MC, Rice CM, Hatzioannou T, Bieniasz PD. 2020. Measuring SARS-CoV-2 neutralizing antibody activity using pseudotyped and chimeric viruses. *J Exp Med* 217:e20201181. <https://doi.org/10.1084/jem.20201181>.
 39. Dillon SM, Guo K, Castleman MJ, Santiago ML, Wilson CC. 2020. Quantifying HIV-1-mediated gut CD4(+) T cell death in the lamina propria aggregate culture (LPAC) model. *Bio Protoc* 10:e3486. <https://doi.org/10.21769/BioProtoc.3486>.
 40. Guo K, Barrett BS, Mickens KL, Hasenkrug KJ, Santiago ML. 2021. Interferon resistance of emerging SARS-CoV-2 variants. *bioRxiv* <https://doi.org/10.1101/2021.03.20.436257>.